

**Immortalized multipotent pericytes derived from the vasa vasorum  
in the injured vasculature.  
A cellular tool for studies of vascular remodeling and regeneration**  
(傷害血管周囲に発生する微小血管 (vasa vasorum) 由来の毛細血管幹細胞株の樹立)

旭川医科大学大学院医学系研究科博士課程医学専攻

**鹿原真樹**

( 川辺淳一、松木孝樹、平 義樹、蓑島暁帆、島村浩平、山内敦司、  
青沼達也、西村正人、斎藤幸裕、竹原有史、長谷部直幸 )

**Immortalized multipotent pericytes derived from the vasa vasorum in the injured vasculature.**

**A cellular tool for studies of vascular remodeling and regeneration**

Maki Kabara<sup>a</sup>, Jun-ichi Kawabe<sup>b\*</sup>,

Motoki Matsuki<sup>a</sup>, Yoshiki Hira<sup>c</sup>, Akiho Minoshima<sup>a</sup>, Kohei Shimamura<sup>a</sup>, Atsushi Yamauchi<sup>a</sup>, Tatsuya Aonuma<sup>a</sup>,

Masato Nishimura<sup>a</sup>, Yukihiro Saito<sup>d</sup>, Naofumi Takehara<sup>b</sup>, and Naoyuki Hasebe<sup>a, b</sup>

a Department of Medicine, Division of Cardiovascular, Respiratory and Neurology

b Department of Cardiovascular Regeneration and Innovation

c Department of Anatomy

d Department of Vascular Surgery

Asahikawa Medical University, Asahikawa, Japan

Short title

**Adventitial Capillary Stem Cell Line**

*Grants;* Funding for this study was provided by a Grant-in-Aid for Scientific Research from the Ministry of Education, Science, Sports, and Culture of Japan (22590820, 25461121)

**\* Corresponding Author; Jun-ichi Kawabe. MD, PhD,**

2-1-1 Midorigaoka-higashi, Asahikawa, 078-8510, Japan

Fax +81-166-68-2449, Tel+81-166-68-2442,

E-mail kawabeju@asahikawa-med.ac.jp

## Abstract

Adventitial microvessels, vasa vasorum in the vessel walls have an active role in the vascular remodeling, although its mechanisms are still unclear. It has been reported that microvascular pericytes (PCs) possess mesenchymal plasticity. Therefore, microvessels would serve as a systemic reservoir of stem cells and contribute to the tissues remodeling. However, most aspects of the biology of multipotent PCs, in particular of pathological microvessels are still obscure because of the lack of appropriate methods to detect and isolate these cells. In order to examine the characteristics of multipotent PCs, we established immortalized cells residing in adventitial capillary growing at the injured vascular walls.

We recently developed *in vivo* angiogenesis to observe adventitial microvessels using collagen-coated tube (CCT), which also can be used as an adventitial microvessel-rich tissue. Using the CCT, CD146- or NG2-positive cells were isolated from the adventitial microvessels in the injured arteries of mice harboring a temperature-sensitive SV40 T antigen gene. Several capillary-derived endothelial cells (cECs) and pericytes (cPCs) cell lines were established. cECs and cPCs maintain a number of key endothelial and pericytes features. Co-incubation of cPC with cECs formed capillary-like structure in Matrigel. Three out of 6 cPCs lines, termed capillary multipotent PCs (mPCs) demonstrated both mesenchymal and neuronal stem cell-like phenotypes, differentiating effectively into adipocytes, osteoblasts as well as schwann cells. mPCs differentiated to ECs and PCs, and formed capillary-like structure on their own. Transplanted DsRed expressing mPCs were resident in the capillary and muscle fibers and promoted angiogenesis and myogenesis in

damaged skeletal muscle. Adventitial mPCs possess trans-differentiation potential with unique phenotypes, including the reconstitution of capillary-like structures.

Their phenotype would contribute to the pathological angiogenesis associated with vascular remodeling. These cell lines also provide a reproducible cellular tool for high-throughput studies on angiogenesis, vascular remodeling, and regeneration as well.

## **Abbreviations**

Pericytes, PCs; Endothelial cells, ECs; glial fibrillary acidic protein, GFAP;

Insulin-like growth factor, IGF; temperature-sensitive SV40, tsSV40; transforming growth factor, TGF; vascular endothelial growth factor, VEGF; von Willebrand factor, vWF.

## **Keywords**

Vasa vasorum, Angiogenesis, Pericytes, Mesenchymal stem cells, Neuronal stem cells

Pericytes (PCs), also known as vascular mural cells, physically surround endothelial cells (ECs) in microvessels, including pre-capillary arterioles, capillaries, and post-capillary venules<sup>1</sup>. PCs regulate the vascular tone, stability, maturation, and remodeling of vessels<sup>1,2</sup>. In addition their angiogenic features, some populations of PCs are defined as multipotent stem cells including mesenchymal stem cells (MSCs)<sup>3,4</sup>, white adipocyte progenitors<sup>5</sup>, skeletal muscle stem cells<sup>6</sup>, and neural stem cells<sup>7</sup>. Because blood vessels are distributed throughout most tissues, multipotent PCs may be a major source of tissue-resident stem cells, which contribute to tissue renewal or remodeling after trauma, diseases, or aging<sup>4</sup>. Commonly used PC markers, including the proteoglycan NG2, platelet-derived growth factor receptor beta (PDGFR $\beta$ ), and CD146, label heterogeneous PC populations<sup>1,2</sup>. To date, no specific marker is available to define the PC phenotype, including multipotent PCs<sup>8,9</sup>. Therefore, most aspects of the biology of multipotent PCs are still obscure because of the lack of appropriate methods to detect and isolate these multipotent PCs.

The tunica adventitia of large blood vessels consisting of the collagen-rich extracellular matrix, stromal cells/fibroblasts, the vasa vasorum, and perivascular nerves, has been recognized just as a passive structural player<sup>10</sup>. However, the importance of the tunica adventitia was recently reevaluated. Adventitial neovascularization is associated with atherosclerotic plaque progression<sup>11-13</sup>. Development of an immature neointimal vasa vasorum results in the delivery of blood substrates, including inflammatory cells and lipids, into plaques and the plaque hemorrhages, thereby contributing to the enlargement of plaque growth and destabilization, which are believed to increase the risk of vessel occlusion<sup>14</sup>. Recent studies have demonstrated

the existence of adventitial stem/progenitor cells, including multipotent PCs as a system reservoir for tissue resident stem cells<sup>15-17</sup>. In a vascular remodeling setting following vascular injury, in parallel with adventitial neovascularization, adventitial progenitor cells start a process of proliferation, migration and differentiation and contribute to vascular remodeling<sup>18, 19</sup>. Therefore, the growing vasa vasorum may serve as a vascular niche for adventitial stem cells, including multipotent PCs, and plays an active role in vascular remodeling<sup>17</sup>.

A transgenic mouse harboring the temperature-sensitive SV40 large T-antigen gene (tsSV40Tg mouse) expresses inactive tsSV40 in all tissues. When the isolated cells are cultured at 33 °C, cells can be easily immortalized by the activation of tsSV40<sup>20</sup>. When the immortalized cells are incubated at temperatures over 37 °C, the tsSV40 is degraded, and the cells exhibit specific phenotypes similar to the original cells. This strategy has been successfully utilized for establishing immortalized cell lines from tissues with small dimensions to clarify the characteristics of certain kind of cells that are somewhat difficult to prepare each time from native tissues. Although PCs are found in capillaries which are distributed throughout most tissues, it is difficult to isolate PCs within the whole tissue, because commonly used PC markers are not PC-specific and differ depending on the tissue and even the developmental stage<sup>4</sup>. Using tsSV40Tg mice, immortalized PC lines have been established only from certain restricted capillary-rich tissues, such as the retina and capillaries isolated from brain tissue<sup>21, 22</sup>. However, PCs from capillaries in other peripheral tissues, especially in the pathological setting, have not been established.

Recently, we have developed a new *in vivo* angiogenesis assay using a collagen-coated tube (CCT) to

observe adventitial microvasculature growing around injured arterial walls<sup>23</sup>. The thin collagen membrane (CCT-membrane), in which microvessels are present at a high density and are distributed two-dimensionally, can be examined quantitatively for adventitial angiogenesis<sup>23</sup>. We noticed that the CCT-membrane can also be used as an ideal microvessel-rich tissue from which we can isolate adventitial capillary cells. In the present study, using the unique CCT method, we successfully established immortalized capillary cells from the growing adventitial microvessels of injured femoral walls of tsSV40Tg mice.

## **MATERIALS AND METHODS**

### **Animals**

Transgenic mice harboring the tsSV40 large T-antigen gene were donated by FACT Co (Sendai, Japan). All animal experiments were performed according to procedures approved by the Animal Care and Use Committee of Asahikawa Medical University.

### **Preparation of CCT-membranes and Cells**

A wire-mediated vascular injury model was generated as described previously<sup>24</sup>. A collagen-coated tube (CCT) was attached just beside the injured femoral artery<sup>23</sup>. Two weeks after the surgery, the collagen-layer on the CCT (CCT-membrane) was removed. The microvessel-rich CCT-membrane was cut into 2-mm pieces and incubated in 500 µg/ml liberase DL (Roche, Basel, Switzerland) in Hanks buffered solution for 30 min at 37 °C. The isolated cells were incubated with Dulbecco's modified Eagle's medium (DMEM) supplemented with 10%

fetal bovine serum (FBS), 100 U/ml penicillin and 100 µg/ml streptomycin at 33 °C in a CO<sub>2</sub> incubator.

### **Isolation of Capillary Cells and Establishment of Cell Lines**

After the cells were sub-cultured for two passages, they were re-suspended in buffer A (phosphate-buffered saline (PBS) containing 0.5% bovine serum albumin (BSA) and 2mM EDTA). To isolate capillary-derived

endothelial cells (cECs) and pericytes (cPCs), the cells were incubated with anti-CD146- or NG2-microbeads.

The microbeads-reacted cells (9.55% CD146+ cells and 6.28% NG2+ cells) were isolated from the total cells

using a magnetic cell sorting system (Miltenyi Biotec, Bergisch Gladbach, Germany). For cECs, CD146<sup>+</sup> cells

were incubated at 33 °C on fibronectin-coated dishes with endothelial basal medium (EBM2; Lonza, Basel,

Switzerland) containing 20 ng/ml vascular endothelial growth factor (VEGF), 10 U/ml heparin, and 10% FBS.

For cPCs, NG2<sup>+</sup> cells were suspended in DMEM containing 10% FBS, and incubated at 33 °C. For the

establishment of cloned cell lines, single cells were seeded in collagen-coated 96-well plates at diluted densities,

and the cells of each formed colony were collected. To trace injected cells within tissues, cells were infected

with a retrovirus harboring the DsRed- or green fluorescent protein (GFP) genes to label living cells.

Fluorescence-expressing cells were sorted using fluorescence activated cell sorting (FACS) flow cytometry

(FACS Aria II, Beckman Coulter Inc, Brea, CA).

### **Reverse Transcription-Polymerase Chain Reaction (RT-PCR) Analysis**

RT-PCR analysis was performed as described previously<sup>25, 26</sup>. Briefly, total RNA was extracted from cells

using the RNeasy Mini Kit (Qiagen, Hilden, Germany). RT-PCR was carried out with the SuperScript

One-Step RT-PCR kit (Invitrogen, Carlsbad, CA) in the presence of 10  $\mu\text{mol/l}$  sense and anti-sense primers.

Sequences of the specific primers are shown in Supplemental Table 1.

### **Gene Microarray Analysis**

For the oligo DNA microarray analysis, RNA samples were collected on day 6 after adipogenesis differentiation

at 37 °C. RNA samples from cells without induction were used as the control. The 3D-Gene Mouse Oligo

Chip 24K (Toray Industries Inc., Tokyo, Japan) was used. The Cy3- or Cy5- labeled aRNA was pooled and

dissolved in hybridization buffer and was hybridized for 16 hr. Hybridization signals were scanned using the

3D-Gene Scanner (Toray Industries) and processed by 3D-Gene Extraction software (Toray Industries). Raw

data intensities greater than 2 standard deviations (SD) of the background signal intensity were considered valid.

The detected signals for each gene were normalized by the global normalization method (Cy3/Cy5 ratio median=1).

### **Flow Cytometry Analysis**

For flow cytometry analysis, cells were suspended in buffer A, incubated with specific primary antibodies, and

then stained with secondary antibodies. The negative control sample was incubated with a non-specific

antibody of the same isotype as the specific primary antibody, and stained with the same secondary antibody.

Cells were analyzed using a flow cytometer (Cytomics FC500TM, Beckman Coulter). The primary antibodies

used in this study include those against CD11b, CD29, CD31, CD34, CD44, CD45, CD73, CD105, CD106,

Sca-1, Fabp4, oligodendrocyte marker O4 (R&D Systems, Minneapolis, MN), NG2, CD146 (Abcam,

Cambridge, UK), alpha smooth muscle actin ( $\alpha$ SMA)(Sigma, St. Louis, MO).

### **Immunohistological Analysis**

The skeletal muscle tissue was embedded in optimal cutting temperature (O.C.T.) compound, and transverse cryosections (10  $\mu$ m) were dried on glass plates. Sections were fixed with 4% paraformaldehyde (PFA)/PBS

for 30 minutes. For immunostaining, the cells were fixed with 2% PFA/PBS for 20 minutes. In particular,

cECs were incubated with DMEM containing 2% BSA and 10 mg/ml

1,1'-dioctadecyl-3,3,3'-tetramethylidocarbocyanine perchlorate-labeled acetylated LDL (DiI-Ac-LDL;

Biogenesis, Mill Creek, WA) at 37 °C for 2 hours before fixation. After fixation, the sample was incubated

with specific primary antibodies at 4 °C overnight, followed by staining with secondary antibodies conjugated to

Alexa Fluor 568 or Alexa Fluor 488 (Invitrogen). The nuclei were counterstained with mounting medium with

Hoechst 33258 (Lonza). Fluorescence images were collected by a (confocal) fluorescence microscope

(Olympus FV1000D and Leica AF6000).

### **Electron Microscopic Observation**

CCT-membranes were fixed and embedded in epoxy resin (Epon812) as described previously<sup>23</sup>. Ultrathin

sections from the tissue blocks embedded in Epon 812 were contrasted with saturated aqueous solutions of

uranyl acetate and lead citrate, and examined with a transmission electron microscope (H-7650, Hitachi High

Technologies, Tokyo, Japan)

### ***In vitro* Differentiation Assay**

Cell differentiation was induced by incubation with appropriate differentiation media according to the manufacturer's manual (Mesenchymal Stem Cell Functional Identification Kit (SC-010) and Neural Lineage Functional Identification Kit (SC-028); R&D Systems). *For adipogenic differentiation*, cells were incubated with  $\alpha$ MEM (Gibco, Carlsbad, CA) containing hydrocortisone, isobutylmethylxanthine and indomethacine, and 10% FBS at 37 °C. After 7-14 days of incubation, cells were fixed and stained with Oil-Red-O (Nacalai Tesque, Kyoto, Japan) or boron-dipyrromethene (BODIPY; Adipocyte Fluorescent Staining Kit, Cosmo Bio, Tokyo, Japan). Adipogenesis-specific genes were immunostained using anti-Fabp4-antibody. *For osteogenic differentiation*, cells were incubated with  $\alpha$ MEM supplemented with ascorbate-phosphate,  $\beta$ -glycerolphosphate and recombinant human BMP-2, and 10% FBS at 37 °C. After 14-21 days, cells were stained with Alizarin-Red (Sigma-Aldrich) or anti-osteopontin antibody (R&D Systems). *For chondrogenesis*, cell pellets were incubated in serum-free DMEM/F-12 (Gibco) containing dexamethasone, ascorbate-phosphate, proline, pyruvate and recombinant human TGF- $\beta$ 3, at 37 °C. After 17-21 days, pellets were stained with anti-collagen 2 (R&D Systems). *For neurogenic differentiation*, cells were pre-treated with base medium (DMEM/F12 plus N-2 Max Media supplement (R&D Systems)) supplemented with recombinant human fibroblast growth factor and human epidermal growth factor for 48 hours on plates coated with poly-L-ornithine and fibronectin. Then, the medium was switched to differentiation medium (base medium plus insulin-like growth factor 1, fetal bovine serum). After 7-10 days of incubation, cells were fixed and stained with each of the following antibodies; anti-nestin-antibody, anti- $\beta$ 3-tubulin-antibody, anti-marker O4-antibody, or anti-S100 $\beta$  antibody. *The in vitro*

*vascular formation assay* was carried out as described previously<sup>23, 26</sup>. Briefly, cells and/or mouse thoracic aorta rings were enclosed in Matrigel (BD Biosciences) and incubated with EMB medium (Lonza) containing 20 ng/ml VEGF. After the indicated incubation time, the cells were extracted and applied to RT-PCR analysis. Some samples were fixed and observed by electron microscopy or immunostaining<sup>23</sup>.

### ***In vivo* differentiation assay**

The *skeletal muscle injury model*, cardiotoxin (Sigma-Aldrich; 100 µl of 0.25 mg/ml in saline per mouse) was injected into the gastrocnemius of SCID mice (age, 8-10 weeks, male). At 4 hours after the surgery or skeletal damage, DsRed-expressing cells ( $1 \times 10^5$  cells in 200 µl saline) were injected into the ischemic or damaged muscles. At 2-3 weeks after cell transplantation, the vascular intraluminal endothelial layer was stained by the infusion of fluorescein isothiocyanate (FITC)-conjugated *Griffonia simplicifolia* (GSA)- lectin (Vector Laboratories, Burlingame, CA) (0.5 mg/ml saline; 300 µl/mouse) via the tail vein just before euthanasia, as described previously<sup>23</sup>.

### **Statistical Analysis**

Unless otherwise indicated, all data represent means  $\pm$  SEM. An unpaired two-tailed Student's t test was used to determine the significance of any differences between two group means.

## RESULTS

### Isolation and Characterization of Adventitial cPCs and cECs

Two weeks after wire-mediated injury in femoral artery, enhanced angiogenesis was observed around the injured femoral artery and on the CCT. Microvessels were observed at high density in the CCT-membrane (Figure 1A). Most NG2-positive cells were observed as mural cells just outside the lectin-stained endothelial tube (Figure 1B), suggesting that NG2 is a good marker for the isolation of microvascular pericytes from the CCT-membrane sample. Single cells within the CCT-membrane were dispersed and cell lines positive for pericyte and endothelial cell markers (NG2 and CD146 respectively) were generated using an immuno-magnetic cell sorting system as described in *Materials and Methods*. Although CD146 are proposed for detection of ECs such as capillary ECs<sup>27</sup>, CD146 is not completely EC-specific, occurring in PCs and smooth muscle cells at low level<sup>28, 29</sup>. Therefore, to obtain cECs, CD146<sup>+</sup> cells from colonies showing a cobble-stone like monolayer appearance were selected. After immortalization and subcloning, six cPC and three cEC lines were obtained from Ts-SV40T mice.

Morphologically, all cPCs appeared to be spindle-fiber shaped and showed a hill-and-valley appearance at confluence (Figure 1C). To confirm the pericyte phenotype, we examined the genetic profile of cPCs by RT-PCR. During long-term culture, *i.e.* 30 passages, cPCs maintained the expression of pericyte-specific marker genes and proteins including NG2, PDGFR $\beta$ , calponin and  $\alpha$ SMA, but not endothelial cell-specific markers such as von Willebrand factor (vWF) and Flk1 genes (Figure 1D & Figure 2). When cPCs were

incubated with the thoracic aorta ring in 3D-Matrigel, they migrated and attached around the sprouting endothelial tubes to form capillary-like structures (Figure 1 E,F).

### ***In vitro* Angiogenic Activities of cECs and cPCs**

cECs grew in a monolayer showing a cobblestone appearance at confluence (Figure 3A), and demonstrated stable gene expression of endothelial cell markers such as vWF and Flk1, but not  $\alpha$ SMA (Figure 3B). Endocytosis and lectin-binding activity are widely exploited to identify ECs in culture<sup>30</sup>. cECs maintained the ability to endocytose DiI-Ac-LDL and bind GSA-lectin (Figure 3C). cECs formed endothelial tube-like structures in Matrigel in the presence of VEGF (Figure 3D). In contrast, cPCs (clone #6) formed cell clusters and in part small funicular structures in Matrigel (Supplemental Figure 1). When cPCs were co-incubated with cECs, cPCs attached around the cEC tubes to form capillary like structure (Supplemental Figure 1). The morphological and functional features of these cells were well maintained for long-term culture (more than 30 passages). This suggests that these cells may serve as a good model to study angiogenesis, especially the interaction between cECs and cPCs.

### **Capillary PCs with Bipotential Mesenchymal and Neuronal Pluripotency**

To select multipotent cPCs among the six established cPC lines, we screened cell lines for their adipogenesis differentiation capacity. Three of the cPC lines demonstrated multipotency. For further study, we investigated the characteristics of cells from one cPC line (clone #3 cPCs, termed capillary multipotent PCs

(mPCs)) that exhibited the highest multipotency among these three cell lines; clone #6 cPCs, which had no multipotent properties, was used as the control differentiated PCs, termed cPC6 without specific specification. mPCs were cultured at 37 °C with the appropriate differentiation medium for the indicated periods. For the *adipogenesis assay*, most of the cells (~95%) were stained with the adipose-specific marker FABP4 and accumulated small oil droplets after the 7-days induction period (Supplemental Figure 2A). Furthermore, after longer (14-day) incubation, these cells differentiated into mature adipocytes, with enlarged oil droplets (Figure 4A). Differentiation toward osteoblasts and chondrocytes was also observed when mPCs were exposed to differentiation stimuli for 3 weeks. In the *osteogenesis assay*, the osteoblast specific marker, osteopontin was initially expressed at 7 days (Supplemental Figure 2B) and obvious calcium accumulation was observed after 21 days of incubation (Figure 4B). For *chondrogenic differentiation*, mPCs were incubated under floating culture conditions, and the cell pellets expressed the chondrocyte-specific marker collagen II (Figure 4C).

Interestingly, mPCs displayed broad and effective differentiation capacity, giving rise to not only the mesodermic lineage but also the neuronal cell lineage. Nestin is well known as a marker for neuronal stem cells. A few cells of control cPC6 were stained with nestin, but most of cells were stained in mPCs although the staining was weak (Supplemental Figure 2C, D). When mPCs were incubated for 48 hours with neural maintenance medium, the immune-staining of nestin was getting stronger (Supplemental Figure 2E). Upon additional incubation with neural differentiation medium containing insulin-like growth factor (IGF) for 7 days, these nestin<sup>+</sup> cells differentiated to Marker O4<sup>+</sup> oligodendrocytes (78.1%), S100β<sup>+</sup> schwann cells/astrocytes

(17.1%) and  $\beta$ 3 tubulin<sup>+</sup> neurons (2.8%) (Figure 4D, E, F), and glial fibrillary acidic protein (GFAP)<sup>+</sup> astrocytes (12.4%) (Supplemental Figure 2F).

The immortalized PCs including mPCs, subcultured more than 30 passages were well grown at constant proliferation rate under low temperature (33 °C) culture condition (Figure 5A). When cPC6 were incubated at temperatures over 37 °C, the tsSV40 is degraded and the cell proliferation was gradually reduced (data not shown). In contrast to cPC6, when mPCs (both short-term (20 passages) and long-term (40 passages) cultured cells) were sub-cultured at 37 °C, the proliferation potency was well maintained at least 10 passages (Figure 5A). After mPCs were incubated in the differentiation mediums for adipogenesis and neurogenesis, Fabp4-positive adipocytes and Marker O4-positive oligodendrocytes were estimated by flow cytometry. As shown in Figure 5B, the differentiation efficiency of adipogenesis and neurogenesis of mPCs were approximately 70 and 55% respectively. Importantly, the differentiation efficiency of both long-term and short-term cultured mPCs was similar. Therefore, we confirmed that main characteristics of mPCs were well maintained for long-term culture condition.

### **mPCs Differentiate Into Endothelial Cells and Form Capillary-Like Structures**

In contrast to cPC6 cells (Supplemental Figure 1), mPCs appeared to be connected by thicker projections, forming capillary-like structures under 3D-Matrigel culture conditions in the presence of VEGF (Figure 6A). This feature was not observed when mPCs were cultured without VEGF (data not shown). Ultra-structural

analysis of gel matrices demonstrated that the accumulated cells formed tube-like structures; however, these capillary-like structures were somewhat immature, the tubular cell-cell connections were loose, and their walls were partially covered by other cells (Figure 6B). After 3 days of incubation with VEGF, the medium was exchanged to fresh medium containing transforming growth factor  $\beta$  (TGF  $\beta$ ) instead of VEGF. The vessel-like structures formed were further enlarged (Figure 6C), constituting CD31-positive tubes fully covered by  $\alpha$ SMA-positive cells (Figure 6D). In parallel assays, RT-PCR analysis of these cells in gel demonstrated that VEGF induced the expression of the mature endothelial cell marker vWF, and enhanced  $\alpha$ SMA expression (Figure 6E, F). These data demonstrate that mPCs differentiate into both endothelial cells and pericytes or smooth muscle cells, and have an ability to form mature vessels on their own.

### ***In vivo* Regeneration Potency of mPCs**

We then determined whether the broad multipotency and potent proangiogenic activity of mPCs translates into improved regeneration in damaged tissues or ischemic tissues *in vivo*. For this purpose, DsRed-expressing mPCs were transplanted intramuscularly into immune-deficient mice subjected to cardiotoxin-mediated muscle injury. Two weeks after transplantation into damaged skeletal muscles, regenerating centrally nucleated myofibers that were stained with DsRed were observed, and interestingly, numerous capillaries within regenerating skeletal muscle area also showed DsRed staining (Figure 7A, B). At higher magnitude view, transplanted cells were engrafted into capillary, mostly composed as either capillary

endothelial cells or perivascular cells (Figure 7C, D).

### **Comprehensive Analysis of Gene Expression Profile of mPCs**

Cloned mPCs and other cPCs stably maintain their features. Therefore, these cell lines, which have different multipotent activities, would be very useful to examine the characteristics of adventitial multipotent PCs. The immortalized cPCs (mPCs and cPC6) were assayed for their antigen expression by flow cytometry and RT-PCR, and showed the expression of pericyte markers (NG2,  $\alpha$ SMA, and CD146), but not endothelial markers were well maintained in both mPCs and cPC6 (Figure 8A, B). To date, no specific marker is available to define the multipotent PC phenotype from among other PCs<sup>8,9</sup>. Therefore, it is interesting to compare gene expression levels between mPCs and non-multipotent cPC6 cells. mPCs expressed mesenchymal stem cell markers (CD29, CD44, CD105, CD106, and Sca1), but not endothelial or hematopoietic markers including CD31, CD34, CD11b, and CD45 (Figure 8C). However, these markers were expressed in both mPCs and cPC6 cells (Figure 8B). We performed microarray analysis of gene expression profiles in mPCs and cPC6 cells. The expression levels of some MSC marker genes were increased in mPCs (Table 1). Interestingly, neural stem cell (NSC) marker genes such as nestin were relatively selective for mPCs compared to cPC6 (Table 1).

## DISCUSSION

### Multipotent PCs Derived from Pathological Neovasculature

In general, cellular surface antigen markers are frequently used as the gold standard for the selection of specific cells of interest within tissues. Cellular markers currently used for PCs, such as NG2 and PDGFR $\beta$ , are not PC-specific and differ depending on the tissue<sup>4,31</sup>. NG2 is a frequently utilized PC marker; however NG2-expressing cells also include oligodendrocytes, skeletal myoblasts, cardiomyocytes, and some neural stem cells<sup>4</sup>. Thus, these markers are only useful for the isolation of PCs from restricted capillary-rich tissue.

Recently, we developed a novel *in vivo* angiogenesis assay using the CCT-membrane<sup>23</sup>. As demonstrated in Figure 1, we found that NG2 is a good marker for PCs in the CCT-membrane. In this study, we isolated NG2-positive cells from growing microvessels in this unique the CCT-membrane and successfully developed immortalized capillary PCs from the adventitial vasa vasorum of the injured femoral artery.

Adventitial vasa vasorum neovascularization mediates vascular remodeling, although the mechanisms that mediate vascular remodeling have not been fully elucidated<sup>12</sup>. A number of studies have demonstrated that the adventitia provides a perivascular niche for stem/progenitor cells that contribute to vascular repair, fibrosis, and atherosclerosis<sup>18,32</sup>. Indeed, the number of multipotent PCs increases in the adventitia of injured femoral arteries, and these cells participate in the restenotic response to arterial injury<sup>33 17</sup>. Consistent with these findings, we established multipotent PCs, which have unique features as discussed below, at a relatively high proportion among immortalized PC lines (3 of 6 lines). Therefore, it is suggested that the mPC is a specific PC subtype

associating with the growing adventitial vasa vasorum and contributes to vascular remodeling.

Numerous studies demonstrated that PCs have several different developmental origins, consisting of heterogeneous populations<sup>4</sup>. In this study, series of cPCs cell lines which have different degree of multipotency clearly demonstrated the existence of heterogeneous PC populations, at least multipotent PCs and non-multipotent PCs. Recently, CD146 has been utilized as marker for multipotent PCs<sup>3</sup>. However, CD146 is not a specific marker for certain multipotent PCs, and no specific markers to isolate multipotent cells prospectively from heterogeneous PC populations have been identified by current research<sup>4</sup>. Therefore, to identify multipotent PCs, researchers have to rely on the lack of markers for other cell lineages including non-endothelial (CD31) and non-hematopoietic (CD34) cells<sup>3</sup>. In this study, we analyzed gene expression profiles among non-multipotent cPCs, cPC6 and multipotent PC (mPCs). Indeed, there were no differences in the expression levels of NG2 and CD146 in mPCs and non-multipotent cPC6 (Figure 8, Table 1).

At this time, it is uncertain whether the ratio of multipotent PCs (three of six cPC) within vasa vasorum in the injured vessels is relatively high or not. The ratio of multipotent PCs among all PCs within microvessels might be varied depend on the kinds of tissues and the condition of tissues, *i.e.* inflammatory / regenerative states. The identification of a specific marker to determine stem/progenitor cells among PCs would be crucial in order to clarify the biology of mPCs. Recently, Birbrair *et al.* demonstrated that PC have been identified as a heterogeneous cell population, nestin-positive and -negative PCs in skeletal muscle<sup>34</sup>. Interestingly, nestin-positive PCs can differentiate to skeletal muscle and neural cells<sup>35</sup>. In this study, we

found that expression of nestin was relatively selective for mPCs compared to cPC6 (Supplemental Figure 2C, D). Furthermore, the gene microarray analysis demonstrated that expression level of nestin was higher in mPCs, compared to cPC6 (Table 1). Therefore, these data well consist with the previous study<sup>35</sup>. Therefore, the cPC cellular library, including mPCs, would be a powerful tool to identify specific markers for native mPCs.

### **mPCs are Capillary-Forming Stem Cells**

A number of studies have demonstrated that vascular resident stem/progenitor cells were observed in small and large vessel walls<sup>15, 18, 36</sup>. In addition to their multi-lineage potential, they exert a potent angiogenic effect through either the adoption of either an endothelial- or a pericyte-like phenotype. Campagnolo *et al.* isolated a population of CD34<sup>+</sup>CD31<sup>-</sup> progenitor cells from the adventitia of human saphenous veins (SVPCs)<sup>37</sup>. SVPCs could be cloned *in vitro* and possessed multipotency for differentiating into mesenchymal cells, including PCs and smooth muscle cells (SMCs). SVPCs have pericyte-like features in mouse hind limbs ischemia, formed cell-cell contacts with ECs, stimulated angiogenesis, and improved flow recovery. Adventitial CD34<sup>+</sup>CD31<sup>-</sup>CD146<sup>-</sup> stem cells (ASCs) showed distinct phenotypes from PCs. However, they acquire a pericyte-like phenotype in the presence of growth factors and contribute to angiogenesis<sup>38</sup>. CD146<sup>+</sup>CD34<sup>-</sup>CD31<sup>-</sup> multipotent PCs also act as PCs and contribute to angiogenesis<sup>3, 33</sup>. Recently, vascular resident endothelial progenitor cells (EPCs) were identified by means of a Hoechst-labeled side population<sup>39</sup>. Vascular resident EPCs differentiate into ECs, and restore blood flow and reconstitute long-term surviving blood

vessels.

To our knowledge<sup>8, 19, 39</sup>, these vascular resident stem cells can differentiate into either ECs or PCs to promote angiogenesis *in vivo*, but cannot acquire both kinds of cells to form capillary-like structures. Although early studies demonstrated that MSCs formed capillary-like structures, composed of an endothelial tube covered by PCs<sup>40, 41</sup>, most prepared MSCs are composed of heterogeneous cell populations that may contain endothelial- and pericyte-progenitor cells or pluripotent stem cells<sup>42</sup>. In this study, clonal mPCs acquired both endothelial- and pericyte-like phenotypes in the presence of VEGF and formed capillary-like structure on their own in Matrigel (Figure 6). When mPCs were transplanted into damaged skeletal muscle tissues, mPCs were assembled into a *de novo* long-lasting functional capillary as endothelial and mural cells *in vivo* (Figure 7).

### **mPCs Exhibit Bipotential Pluripotency**

In this study, clonal mPCs exhibit multi-lineage potential, showing the ability to differentiate *in vitro* into both mesenchymal and neuronal lineage cells (Figure 4). This trans-differentiation across germ layers has been previously demonstrated in perivascular stem/progenitor cells<sup>19, 37, 38</sup>. It is widely believed that MSCs are derived from mesoderm. Recent advances in cellular imaging and lineage tracing techniques indicated that MSCs have several different embryonic origins, such as the neural crest, in addition to mesoderm<sup>43, 44</sup>. Neural crest cells are migratory stem cells that are generated along the entire vertebrate axis at the neural plate border, and begin to migrate to the periphery and differentiate into various tissues during development. In adults, stem

cells originating from the neural crest show persistent mesodermal and neuronal differentiation potential, and replenish associated tissues<sup>45</sup>. It is uncertain whether adventitial mPCs originate from neural crest cells.

However, the genomic expression profile of mPCs indicated that some neural stem cell markers, including nestin, are dominantly expressed in these cells compared to control cPC6 (Table 1) as discussed previously.

Perivascular adipose tissues (PAT) have been considered solely as vessel-supporting connective tissue.

A number of recent studies demonstrated that PAT affect the functions of PAT-adjacent vasculature and contribute to vascular remodeling<sup>46, 47</sup>. Adipocytes originally differentiate from adipocyte progenitors and are related to the remodeling of adipose tissues under certain local and general conditions. MSCs residing in the perivascular region depots form and give rise to resident adipocyte progenitors<sup>5</sup>. In this study, we demonstrate that among the various differentiation potencies, the adipogenesis potential of mPCs is relatively high (Figure 4, Supplemental Figure 2). They can differentiate into adipocytes not only at high ratios but also with a high degree of maturation for differentiation. Adventitial mPCs would represent an adipocyte-progenitor feature for the reconstitution of PAT and provide a useful tool to elucidate perivascular adipose development.

In conclusion, we established immortalized capillary cells (ECs and PCs) derived from pathological neovasculature within the adventitia, using the unique CCT-membrane. Especially, we identified mPCs, which have unique multipotent features. Of course, prudent interpretations of the role of these cells should be required as these cell lines were generated by the action of immortalizing the tsSV40. Importantly, genomic

expression profile, cellular functions and immunostaining pattern that are similar to common features of ECs and PCs were well maintained for long-term culture condition. Therefore, these cloned cell lines would be a useful tool for elucidating the characteristics of multipotent PCs and also the interaction between ECs and PCs to form capillary structure.

## **ACKNOWLEDGEMENTS**

We thank K. Kanno, A. Oda, S. Takahashi, Y. Horikawa, and E. Shinokawa for laboratory assistance, and Y.

Segawa for secretarial assistance. *Grants*; Funding for this study was provided by a Grant-in-Aid for

Scientific Research from the Ministry of Education, Science, Sports, and Culture of Japan (22590820,

25461121); a grant from The Akiyama Life Science Foundation, Suhara Memorial Foundation, and Mitsubishi

Pharma Research Foundation.

## **DISCLOSURE/CONFLICT OF INTEREST**

The authors declare no conflict of interest.

Supplementary information is available at Laboratory Investigation's website.

## REFERENCES

- 1 Diaz-Flores L, Gutierrez R, Madrid JF, et al. Pericytes. Morphofunction, interactions and pathology in a quiescent and activated mesenchymal cell niche. *Histology and histopathology* 2009;24(7):909-969.
- 2 Armulik A, Abramsson A, Betsholtz C. Endothelial/pericyte interactions. *Circulation research* 2005;97(6):512-523.
- 3 Crisan M, Yap S, Casteilla L, et al. A perivascular origin for mesenchymal stem cells in multiple human organs. *Cell stem cell* 2008;3(3):301-313.
- 4 Armulik A, Genove G, Betsholtz C. Pericytes: developmental, physiological, and pathological perspectives, problems, and promises. *Developmental cell* 2011;21(2):193-215.
- 5 Tang W, Zeve D, Suh JM, et al. White fat progenitor cells reside in the adipose vasculature. *Science* 2008;322(5901):583-586.
- 6 Dellavalle A, Sampaolesi M, Tonlorenzi R, et al. Pericytes of human skeletal muscle are myogenic precursors distinct from satellite cells. *Nature cell biology* 2007;9(3):255-267.
- 7 Dore-Duffy P, Katychew A, Wang X, et al. CNS microvascular pericytes exhibit multipotential stem cell activity. *Journal of cerebral blood flow and metabolism : official journal of the International Society of Cerebral Blood Flow and Metabolism* 2006;26(5):613-624.
- 8 Chen WC, Park TS, Murray IR, et al. Cellular kinetics of perivascular MSC precursors. *Stem cells international* 2013;2013:983059.
- 9 Murray IR, West CC, Hardy WR, et al. Natural history of mesenchymal stem cells, from vessel walls to culture vessels. *Cellular and molecular life sciences : CMLS* 2013.
- 10 Hildebrandt HA, Gossel M, Mannheim D, et al. Differential distribution of vasa vasorum in different vascular beds in humans. *Atherosclerosis* 2008;199(1):47-54.

- 11 Langheinrich AC, Michniewicz A, Sedding DG, et al. Correlation of vasa vasorum neovascularization and plaque progression in aortas of apolipoprotein E(-/-)/low-density lipoprotein(-/-) double knockout mice. *Arteriosclerosis, thrombosis, and vascular biology* 2006;26(2):347-352.
- 12 Doyle B, Caplice N. Plaque neovascularization and antiangiogenic therapy for atherosclerosis. *Journal of the American College of Cardiology* 2007;49(21):2073-2080.
- 13 Tanaka K, Nagata D, Hirata Y, et al. Augmented angiogenesis in adventitia promotes growth of atherosclerotic plaque in apolipoprotein E-deficient mice. *Atherosclerosis* 2011;215(2):366-373.
- 14 Mulligan-Kehoe MJ. The vasa vasorum in diseased and nondiseased arteries. *American journal of physiology Heart and circulatory physiology* 2010;298(2):H295-305.
- 15 Majesky MW, Dong XR, Hognlund V, et al. The adventitia: a dynamic interface containing resident progenitor cells. *Arteriosclerosis, thrombosis, and vascular biology* 2011;31(7):1530-1539.
- 16 Bautch VL. Stem cells and the vasculature. *Nature medicine* 2011;17(11):1437-1443.
- 17 Kawabe J, Hasebe N. Role of the vasa vasorum and vascular resident stem cells in atherosclerosis. *BioMed research international* 2014;2014:701571.
- 18 Tilki D, Hohn HP, Ergun B, et al. Emerging biology of vascular wall progenitor cells in health and disease. *Trends in molecular medicine* 2009;15(11):501-509.
- 19 Tang Z, Wang A, Yuan F, et al. Differentiation of multipotent vascular stem cells contributes to vascular diseases. *Nature communications* 2012;3:875.
- 20 Obinata M. Conditionally immortalized cell lines with differentiated functions established from temperature-sensitive T-antigen transgenic mice. *Genes to cells : devoted to molecular & cellular mechanisms* 1997;2(4):235-244.

- 21 Kondo T, Hosoya K, Hori S, et al. Establishment of conditionally immortalized rat retinal pericyte cell lines (TR-rPCT) and their application in a co-culture system using retinal capillary endothelial cell line (TR-iBRB2). *Cell structure and function* 2003;28(3):145-153.
- 22 Shimizu F, Sano Y, Maeda T, et al. Peripheral nerve pericytes originating from the blood-nerve barrier expresses tight junctional molecules and transporters as barrier-forming cells. *Journal of cellular physiology* 2008;217(2):388-399.
- 23 Asanome A, Kawabe J, Matsuki M, et al. Nerve growth factor stimulates regeneration of perivascular nerve, and induces the maturation of microvessels around the injured artery. *Biochemical and biophysical research communications* 2014;443(1):150-155.
- 24 Kawabe J, Yuhki K, Okada M, et al. Prostaglandin I2 promotes recruitment of endothelial progenitor cells and limits vascular remodeling. *Arteriosclerosis, thrombosis, and vascular biology* 2010;30(3):464-470.
- 25 Yamauchi A, Kawabe J, Kabara M, et al. Apurinic/aprimidinic endonuclease 1 maintains adhesion of endothelial progenitor cells and reduces neointima formation. *American journal of physiology Heart and circulatory physiology* 2013;305(8):H1158-1167.
- 26 Aburakawa Y, Kawabe J, Okada M, et al. Prostacyclin stimulated integrin-dependent angiogenic effects of endothelial progenitor cells and mediated potent circulation recovery in ischemic hind limb model. *Circulation journal : official journal of the Japanese Circulation Society* 2013;77(4):1053-1062.
- 27 Middleton J, Americh L, Gayon R, et al. A comparative study of endothelial cell markers expressed in chronically inflamed human tissues: MECA-79, Duffy antigen receptor for chemokines, von Willebrand factor, CD31, CD34, CD105 and CD146. *The Journal of pathology* 2005;206(3):260-268.
- 28 Bardin N, Frances V, Lesaule G, et al. Identification of the S-Endo 1 endothelial-associated antigen. *Biochemical and biophysical research communications* 1996;218(1):210-216.
- 29 Wilkinson FL, Liu Y, Rucka AK, et al. Contribution of VCAF-positive cells to neovascularization and

calcification in atherosclerotic plaque development. *The Journal of pathology* 2007;211(3):362-369.

- 30 Laitinen L. Griffonia simplicifolia lectins bind specifically to endothelial cells and some epithelial cells in mouse tissues. *The Histochemical journal* 1987;19(4):225-234.
- 31 Crisan M, Corselli M, Chen WC, et al. Perivascular cells for regenerative medicine. *Journal of cellular and molecular medicine* 2012;16(12):2851-2860.
- 32 Tintut Y, Alfonso Z, Saini T, et al. Multilineage potential of cells from the artery wall. *Circulation* 2003;108(20):2505-2510.
- 33 Tigges U, Komatsu M, Stallcup WB. Adventitial pericyte progenitor/mesenchymal stem cells participate in the restenotic response to arterial injury. *Journal of vascular research* 2013;50(2):134-144.
- 34 Birbrair A, Zhang T, Wang ZM, et al. Type-1 pericytes participate in fibrous tissue deposition in aged skeletal muscle. *American journal of physiology Cell physiology* 2013;305(11):C1098-1113.
- 35 Birbrair A, Zhang T, Wang ZM, et al. Skeletal muscle pericyte subtypes differ in their differentiation potential. *Stem cell research* 2013;10(1):67-84.
- 36 Kovacic JC, Boehm M. Resident vascular progenitor cells: an emerging role for non-terminally differentiated vessel-resident cells in vascular biology. *Stem cell research* 2009;2(1):2-15.
- 37 Campagnolo P, Cesselli D, Al Haj Zen A, et al. Human adult vena saphena contains perivascular progenitor cells endowed with clonogenic and proangiogenic potential. *Circulation* 2010;121(15):1735-1745.
- 38 Corselli M, Chen CW, Sun B, et al. The tunica adventitia of human arteries and veins as a source of mesenchymal stem cells. *Stem cells and development* 2012;21(8):1299-1308.
- 39 Naito H, Kidoya H, Sakimoto S, et al. Identification and characterization of a resident vascular

stem/progenitor cell population in preexisting blood vessels. *The EMBO journal* 2012;31(4):842-855.

40 Pasquinelli G, Tazzari PL, Vaselli C, et al. Thoracic aortas from multiorgan donors are suitable for obtaining resident angiogenic mesenchymal stromal cells. *Stem cells* 2007;25(7):1627-1634.

41 Zorzi P, Aplin AC, Smith KD, et al. Technical Advance: The rat aorta contains resident mononuclear phagocytes with proliferative capacity and proangiogenic properties. *Journal of leukocyte biology* 2010;88(5):1051-1059.

42 Oswald J, Boxberger S, Jorgensen B, et al. Mesenchymal stem cells can be differentiated into endothelial cells in vitro. *Stem cells* 2004;22(3):377-384.

43 Takashima Y, Era T, Nakao K, et al. Neuroepithelial cells supply an initial transient wave of MSC differentiation. *Cell* 2007;129(7):1377-1388.

44 Morikawa S, Mabuchi Y, Niibe K, et al. Development of mesenchymal stem cells partially originate from the neural crest. *Biochemical and biophysical research communications* 2009;379(4):1114-1119.

45 Takahashi Y, Sipp D, Enomoto H. Tissue interactions in neural crest cell development and disease. *Science* 2013;341(6148):860-863.

46 Chang L, Milton H, Eitzman DT, et al. Paradoxical roles of perivascular adipose tissue in atherosclerosis and hypertension. *Circulation journal : official journal of the Japanese Circulation Society* 2013;77(1):11-18.

47 Shimabukuro M, Kozuka C, Taira S, et al. Ectopic fat deposition and global cardiometabolic risk: new paradigm in cardiovascular medicine. *The journal of medical investigation : JMI* 2013;60(1-2):1-14.

## **Titles and legends to figures**

**Figure 1** Characteristics of capillary-derived pericyte (cPCs). **(A)** Numerous microvessels were distributed on the collagen-coated tube (CCT). **(B)** Most NG2-positive cells (red) were located adjacent to the FITC-conjugated lectin-bound endothelial tubes (green) of microvasculature in the CCT-membrane. Nuclei were counterstained with Hoechst 33258. **(C)** At confluence, cPCs developed a classic hill-and-valley morphology. **(D)** RT-PCR shows the expression of typical pericyte-specific markers (1-5) but not endothelial cell-markers (6 and 7) in cPCs. **(E & F)** GFP-expressing cPCs (green) were co-incubated with aorta rings in Matrigel. cPCs were attached around the CD31-stained endothelial tube (red) to form capillary-like structures. Scale bars, 50  $\mu\text{m}$  (**A, B**) and 100  $\mu\text{m}$  (**C, E, F**).

**Figure 2** Expression of pericyte markers in cPCs. At the cells reached to confluent, the cells were fixed and immunostained with antibodies against NG2 (**A**), PDGFR $\beta$  (**B**),  $\alpha$ SMA (**C**), and calponin (**D**). Nuclei were identified by Hoechst 33258 (blue). Scale bars, 50  $\mu\text{m}$ .

**Figure 3** Characteristics of capillary-derived endothelial cells (cECs). **(A)** cECs developed a cobble-stone morphology at confluence. **(B)** Total RNA of cECs was analyzed by RT-PCR and gene expression of the indicated endothelial markers (1-3) but no pericyte marker (4) was observed. **(C)** cECs were incubated with DiI-labeled AcLDL and FITC-conjugated GSA-lectin. cECs maintained the ability to endocytose AcLDL

particles (red) and bind to lectin (green). Nuclei were visualized by DAPI staining (blue). **(D)** cECs were incubated with VEGF in Matrigel, and formed peculiar endothelial tubes (EC-tubes). Axial view of the formed EC-tube is shown (*inset*). Scale bars, 100  $\mu\text{m}$  (**A, D**) and 30  $\mu\text{m}$  (**C**).

**Figure 4** Multipotency of cPCs. Under appropriate differentiation conditions, multipotent PCs (mPCs), one of the established cPC lines (cone #3 PC), displayed broad differentiation capacity. mPCs gave rise to cells of mesodermal lineage such as Oil-Red-stained adipocytes (**A**), Alizarin Red-stained osteoblasts (**B**), and collagen II-immunostained chondrocytes (**C**). mPCs also differentiated into neuronal cells, immunostained with each oligodendrocyte marker O4 (**D**), S100 $\beta$  (**E**), and  $\beta$ 3-tubulin (**F**). Nuclei were identified by Hoechst 33258 (blue). Scale bars, 50  $\mu\text{m}$ .

**Figure 5** Differentiation efficiency of mPCs. **(A)** Cumulative cell numbers during passage under culture at different temperature. Culture of immortalized cells was maintained at 33  $^{\circ}\text{C}$  (open circle). The constant growth rate is maintained for more than 50 passages. In parallel with this maintenance culture, the cells at indicated passage were sub-cultured at 38  $^{\circ}\text{C}$  (closed circle). **(B)** the cells which were sub-cultured at low (20) and high (40) passages were incubated with adipo- and neuro-differentiating medium for 7 days, and differentiated adipocytes or oligodendrocytes were determined by flow cytometry using specific antibodies against Fabp4 and Marker O4 respectively. Negative control was obtained using isotype-matched nonimmune

antibodies.

**Figure 6** mPCs form Capillary-like structures. (A) mPCs formed capillary-like structures in Matrigel in the presence of VEGF. (B) Electron microscopic analysis demonstrated that the formed tubule structure was composed of cellular walls with loose intercellular adhesions. (C) When the gels were further incubated with TGF $\beta$  instead of VEGF, the vessels became thicker. (D) *In situ* immunostaining of Matrigel and confocal microscopic analysis show that the formed vessels are composed of CD31-positive tubules (green) surrounded by  $\alpha$ SMA-positive cells (red). (E) Gene expression of  $\alpha$ SMA and vWF in the presence or absence of VEGF was estimated by RT-PCR. Glyceraldehyde-3-phosphate dehydrogenase (G3PDH) was used as an internal control. (F) The level of each gene in the absence (open bars) or presence (closed bars) was calculated as the ratio to the density of G3PDH. Values are mean  $\pm$  SEM. n=5, \*p<0.05. Scale bars, 200  $\mu$ m (A, C), 10  $\mu$ m (B) and 50  $\mu$ m (D)

**Figure 7** *In vivo* Regenerative Capacity of mPCs. (A) After gastrocnemius of SCID mouse were damaged by cardiotoxin, Ds-Red-mPCs were transplanted into the damaged muscle by intramuscular injection. After 14 days of cardiotoxin-induced muscle damage/cell transplantation, mPCs were well engrafted into regenerative skeletal muscle, composed of myofibers and capillaries as seen in the long and short axial views, respectively (A, B). Confocal microscopic analysis showed that transplantation, mPCs (red) were closely associated with

muscular capillary tubes (green) as endothelial and perivascular cells (**C, D**). Scale bars, 50  $\mu\text{m}$  (**A, B**), and 100  $\mu\text{m}$  (**C, D**).

**Figure 8** Gene and protein expression profile of mPCs and control cPC6. (**A**) Histogram shows flow cytometry analysis of cells enriched with pericyte-surface markers (NG2,  $\alpha$ SMA, CD146), but not endothelial marker, CD31. Signals for fluorescent isotype IgG are shown in black and antigen-specific signals are shown in closed shaded curves. (**B**) Expression levels of indicated genes (1. CD146, 2. NG2, 3. vWF, 4. Flk1, 5. PDGFR $\beta$ , 6.  $\alpha$ SMA and 7. G3PDH) within each PCs cell lines were determined by RT-PCR. (**C**) Cell surface markers for mesenchymal stem cells (CD29, CD44, CD105, CD106 and Sca1), and hematopoietic cells (CD34, CD11b, CD45) of each cell line was determined by flow cytometry.

## Table

### Table 1 Comparison of Gene Expression in cPCs cell Lines.

Gene-expression analysis on cPC cell lines (clone #3 and #6) was done using 3D-Gene mouse Oligo Chip

(Toray). Fold-change difference in gene expression between mPCs (cPC3) and non-multipotent cPCs (cPC6)

was expressed as  $\log_2$  (ratio). PC, pericytes; EC, endothelial cell; MSC, mesenchymal stem cell; NSC,

neuronal stem cell.

**Figure 1**

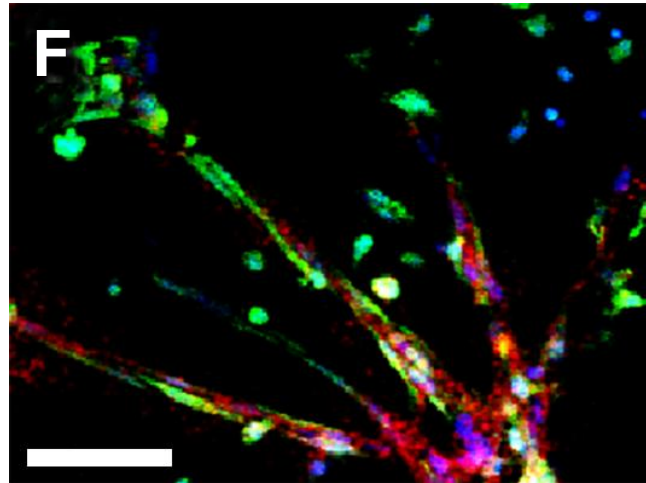
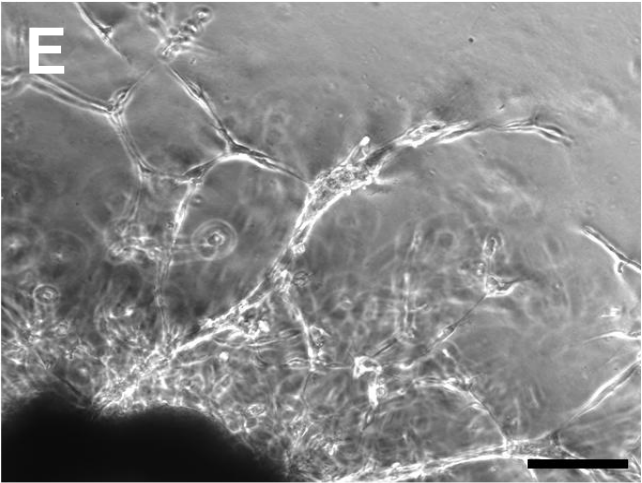
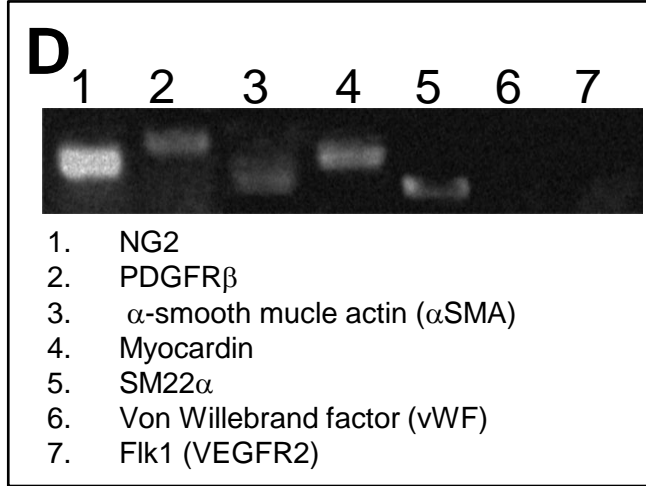
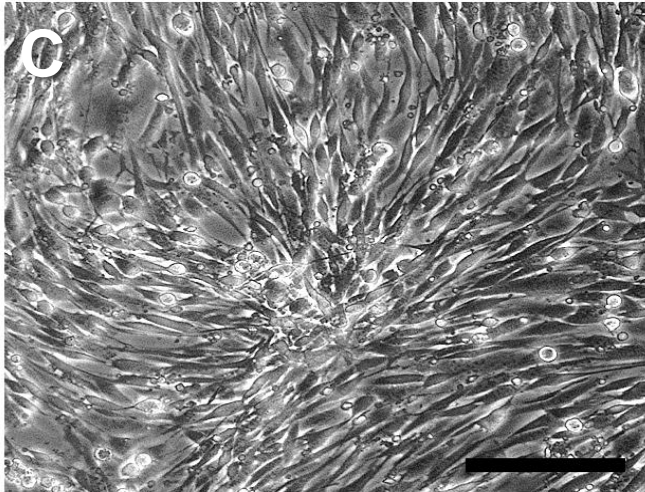
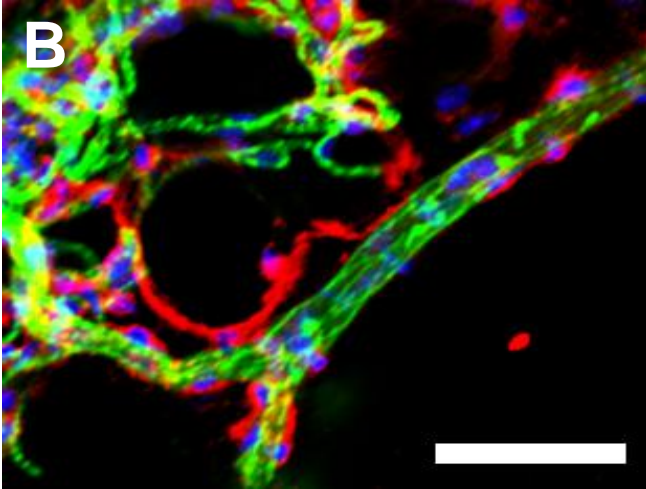
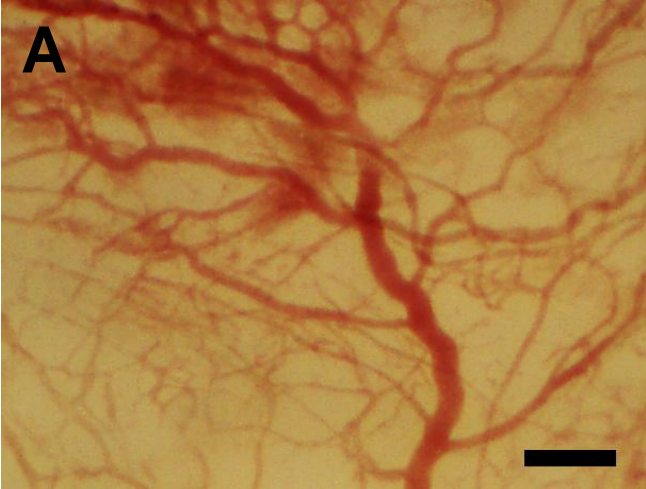


**Figure 2**

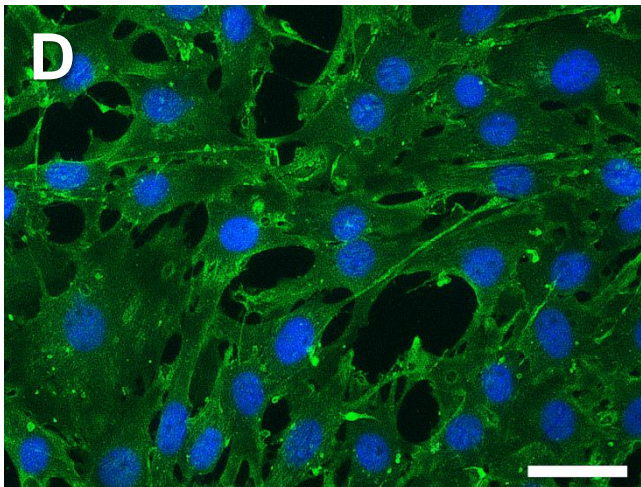
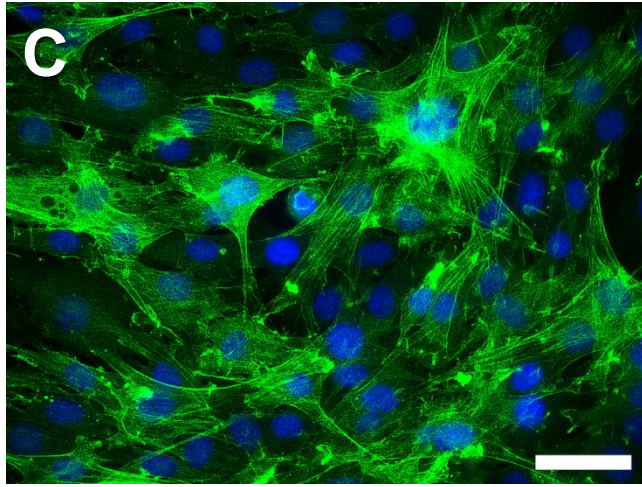
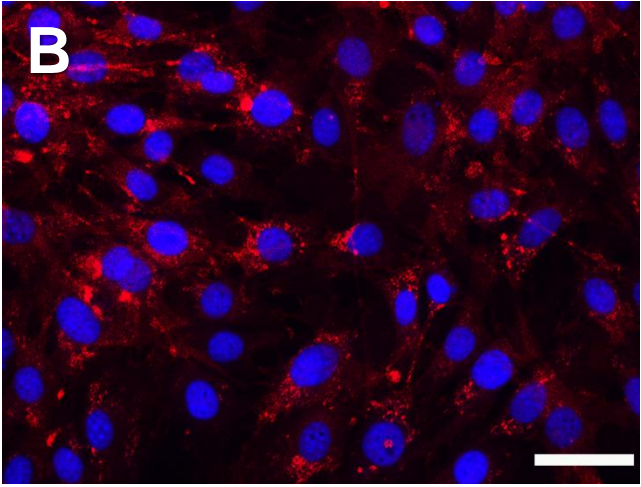
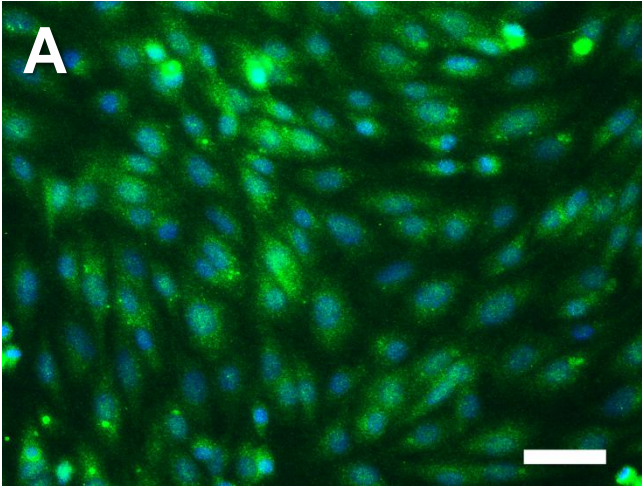


**Figure 3**

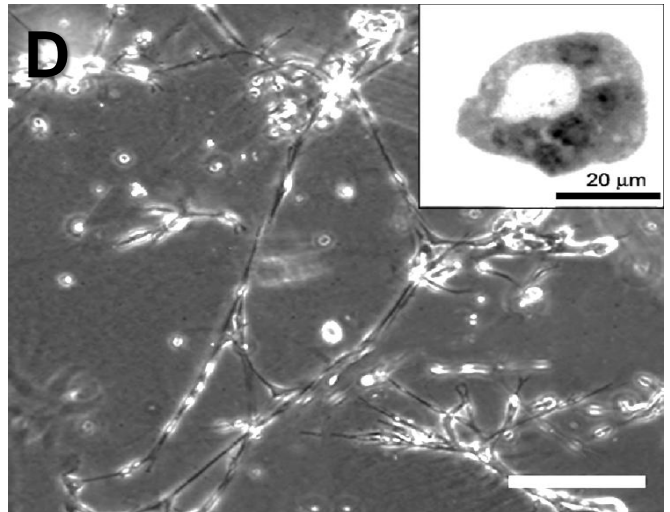
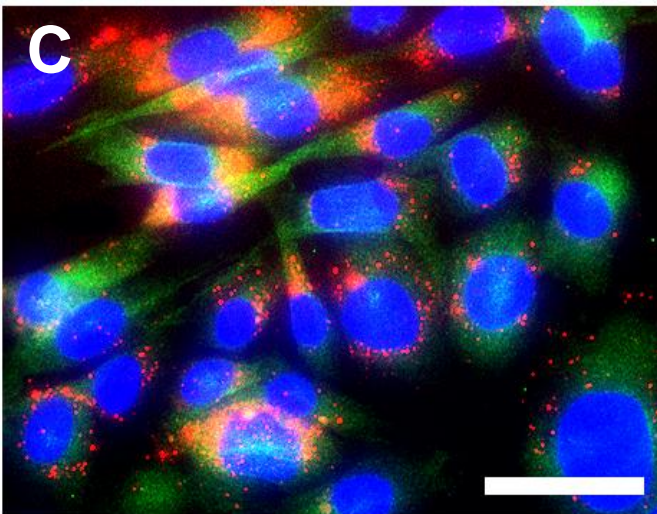
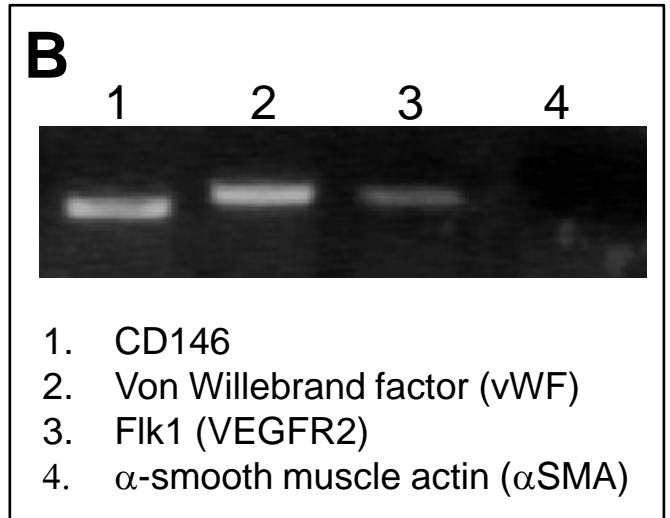
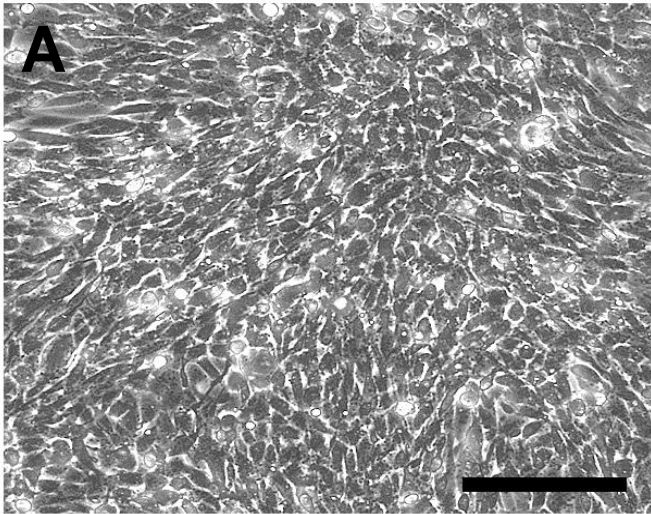


**Figure 4**

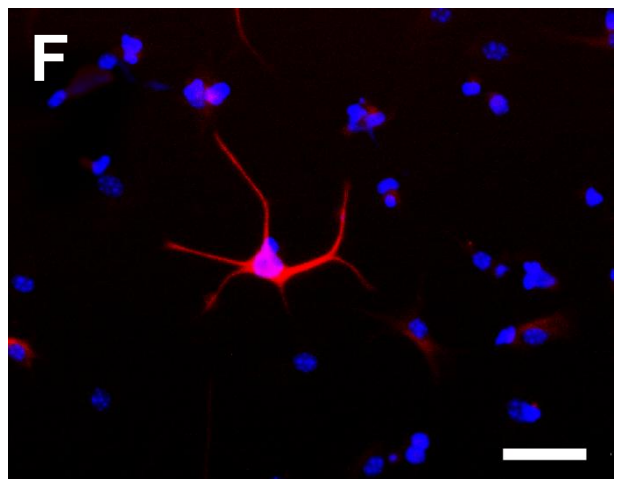
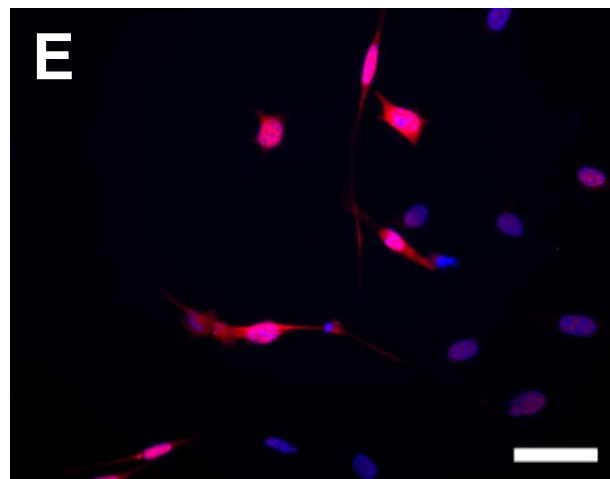
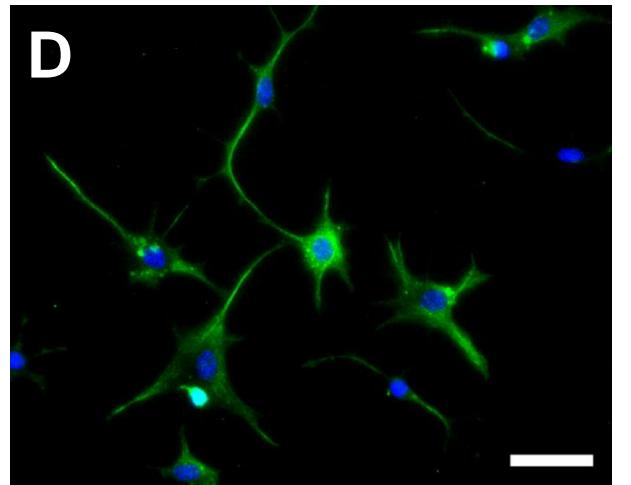
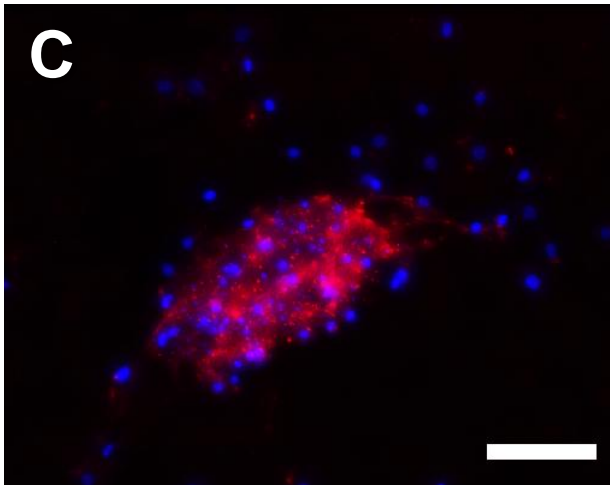
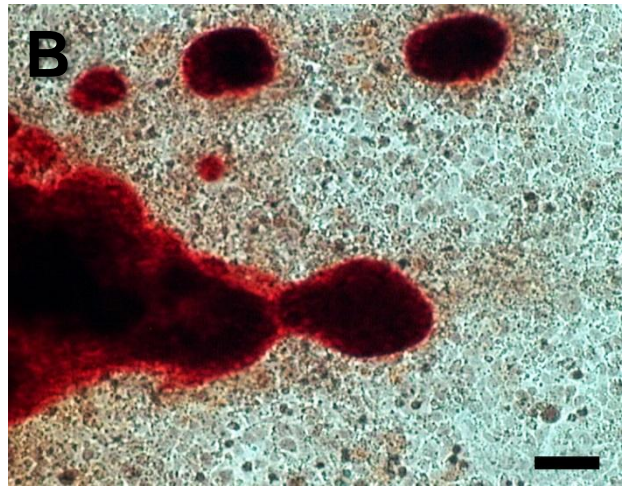
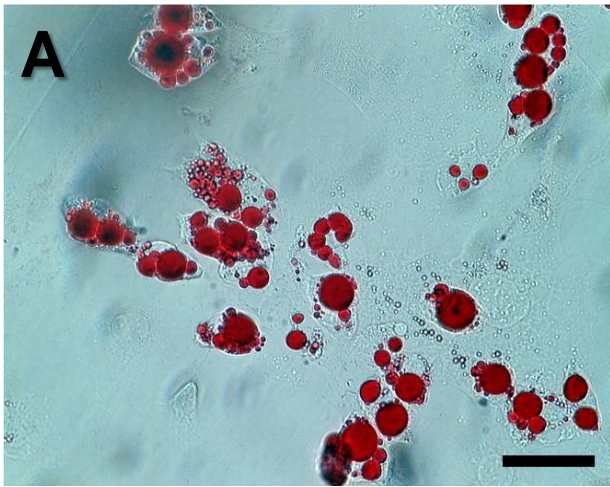
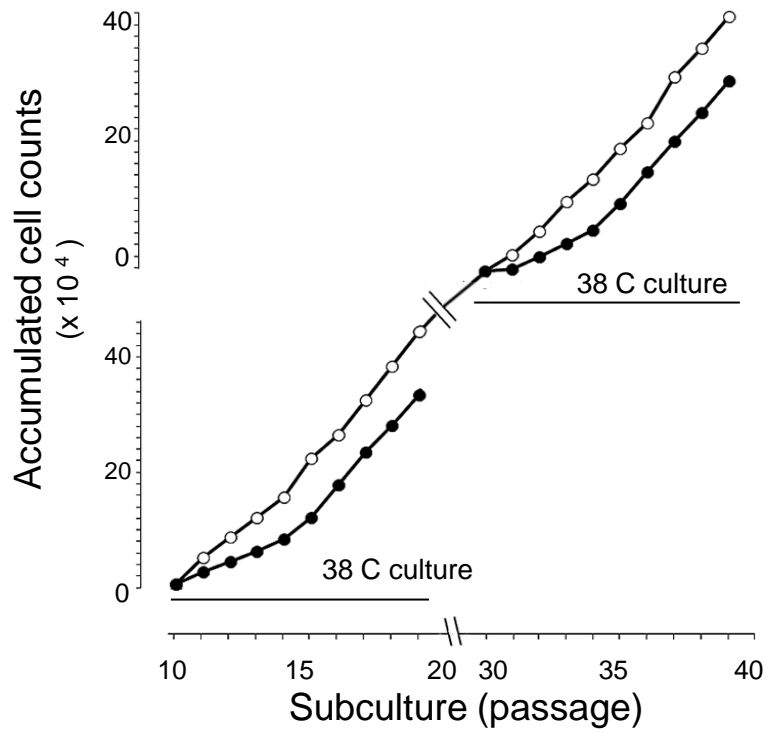


**Figure 5**  
**A**



**B**

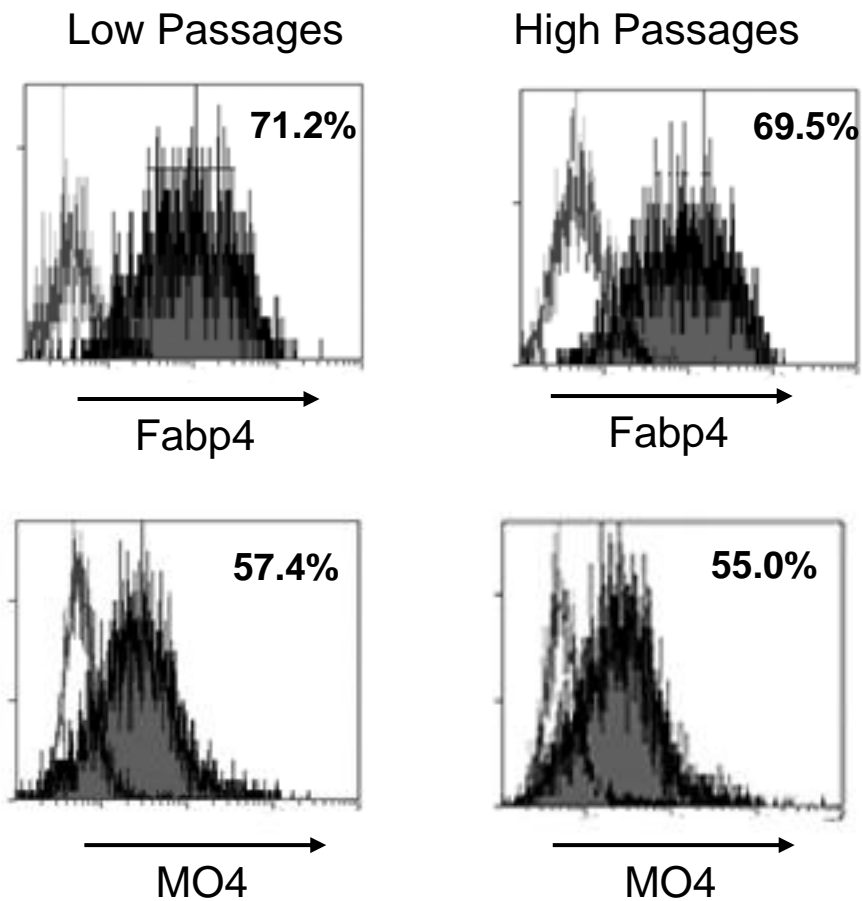


**Figure 6**

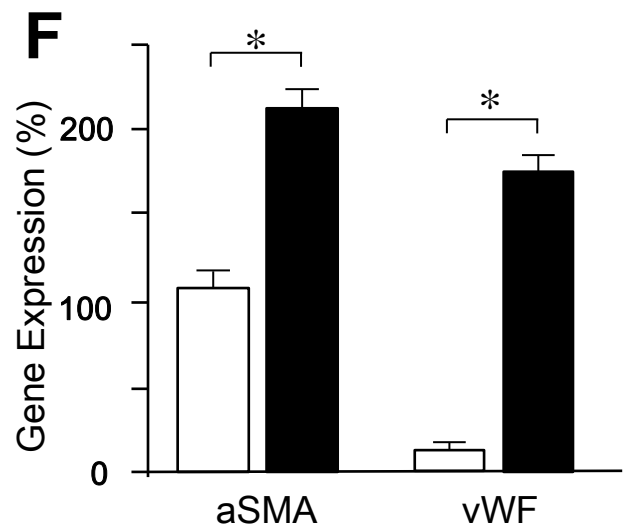
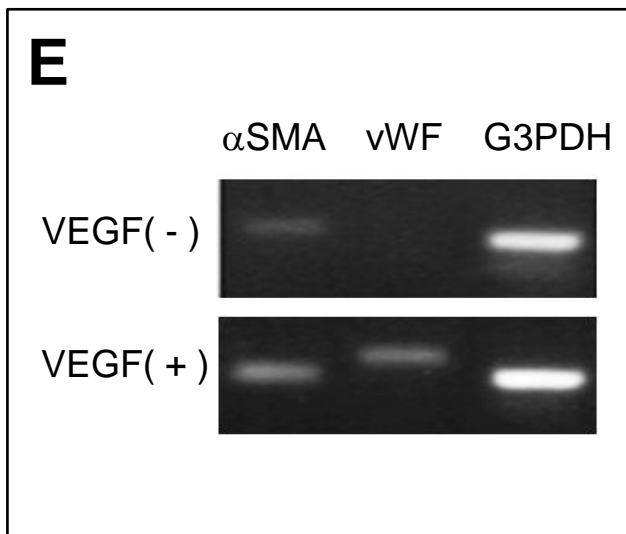
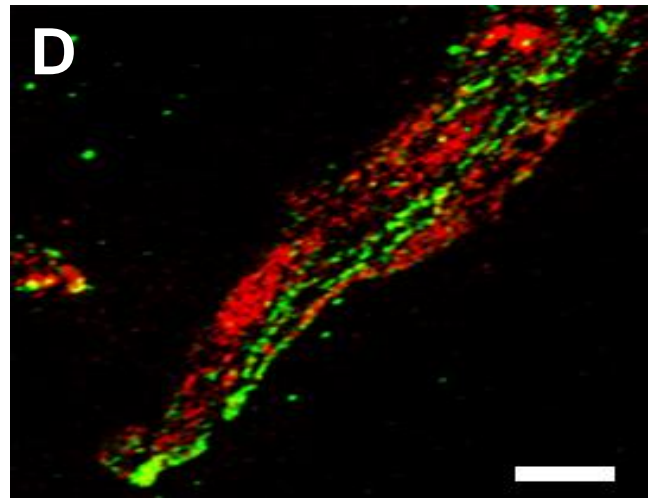
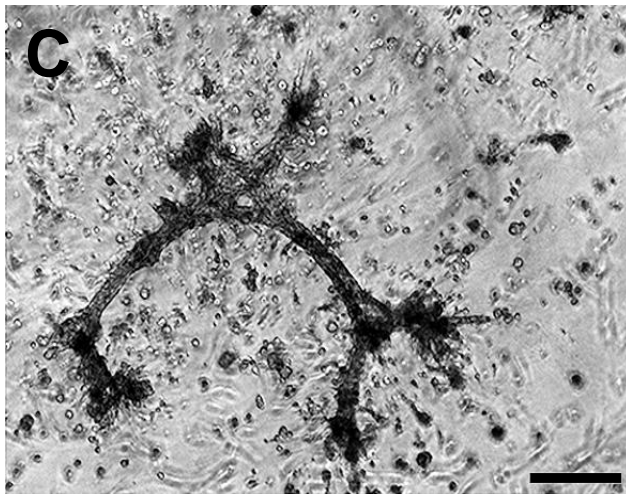
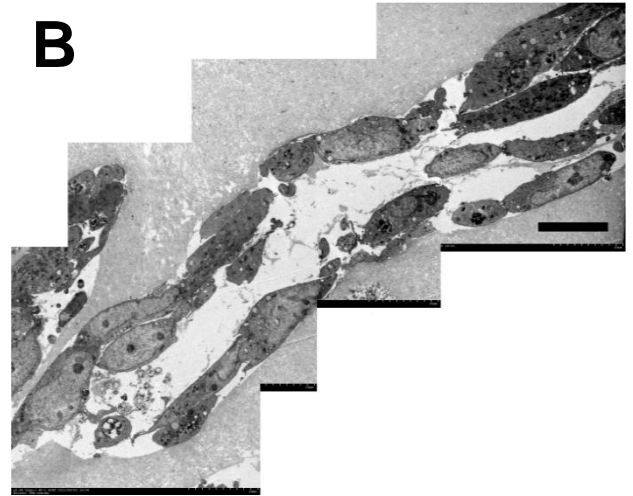
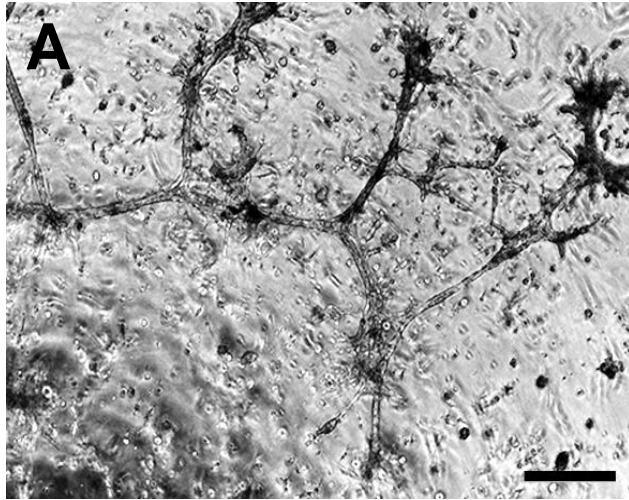


**Figure 7**

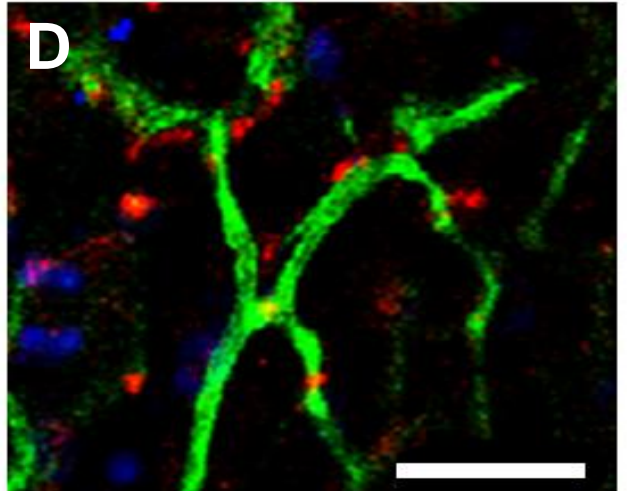
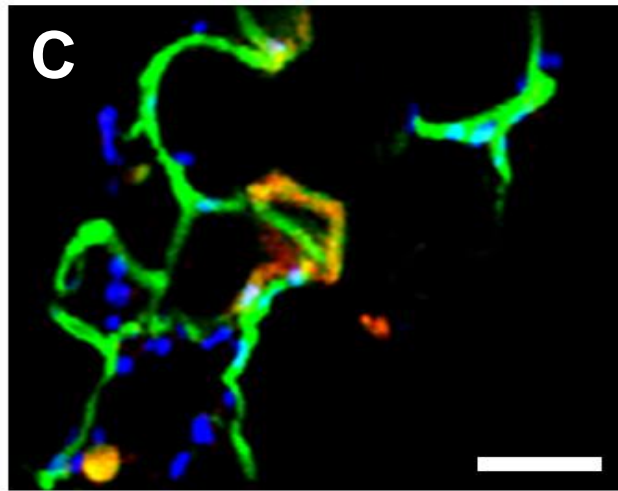
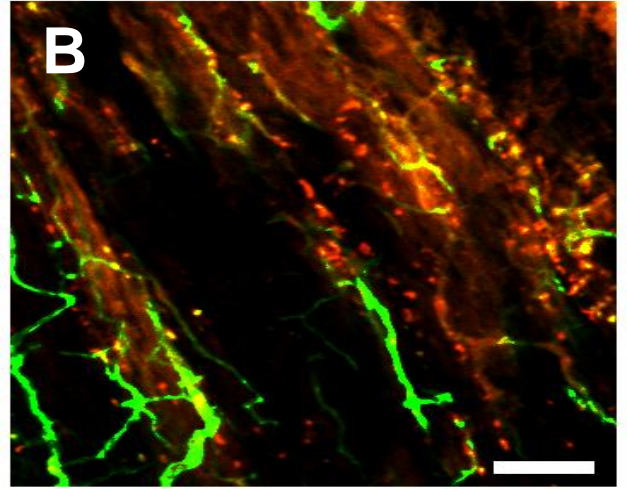
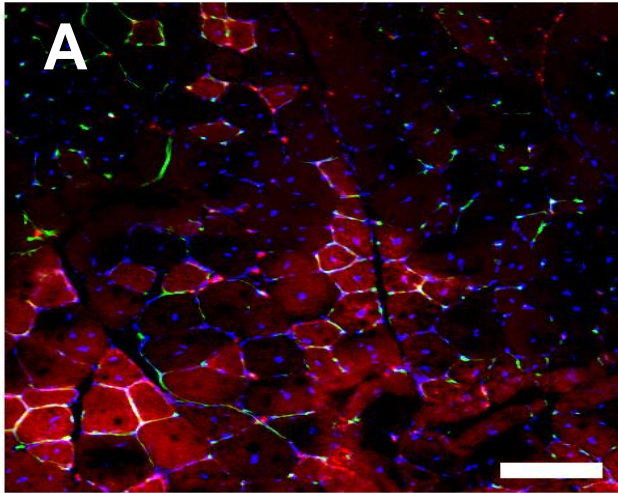
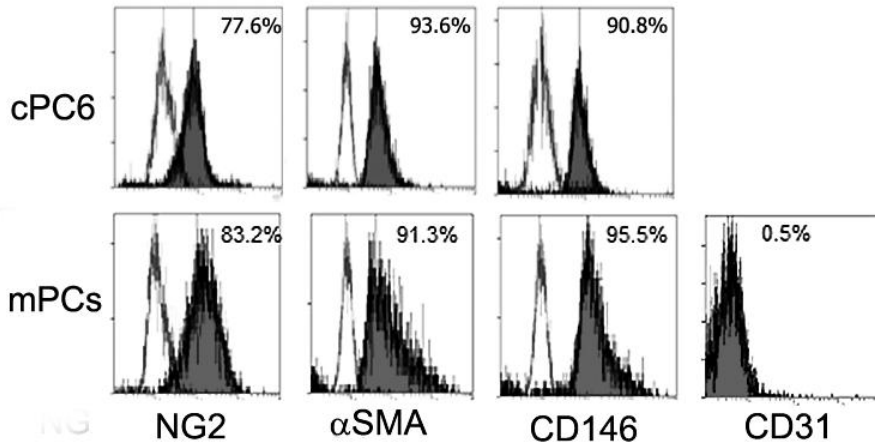
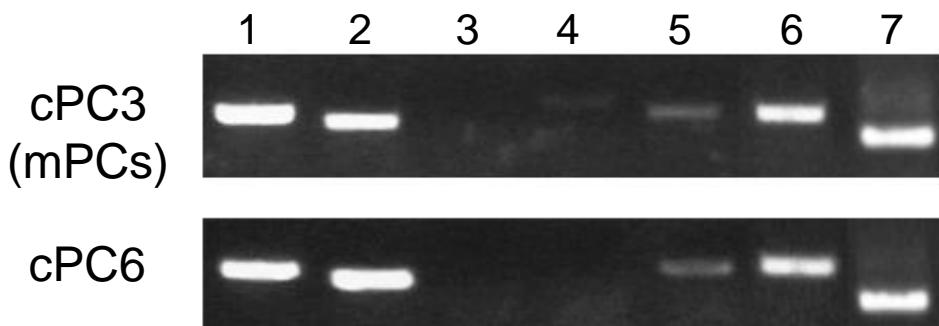


**Figure 8**

**A**



**B**



**C**

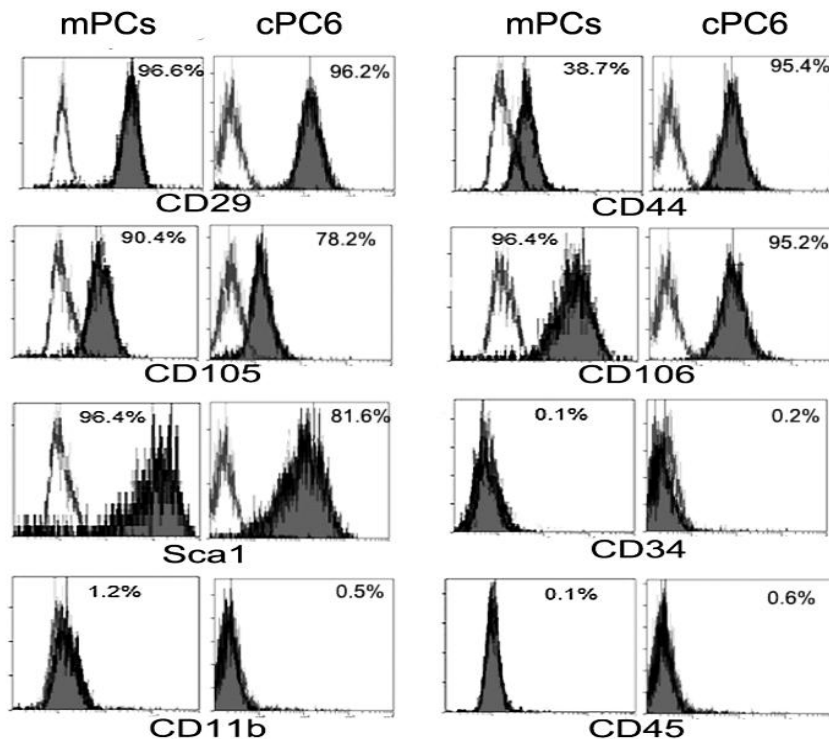


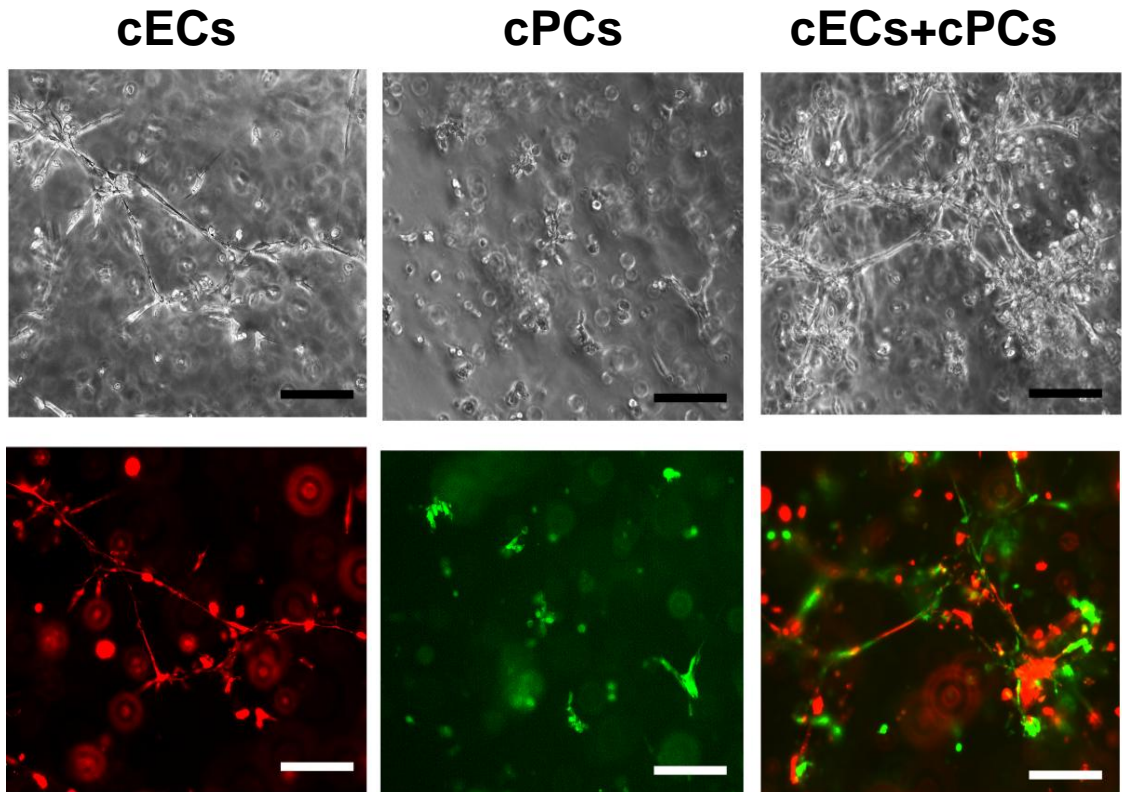
**Table 1**

| Marker   | Gene              | GeneBank<br>accession numbers | cPC3<br>(mPCs) | cPC6  | Difference<br>Log2(ratio) |
|----------|-------------------|-------------------------------|----------------|-------|---------------------------|
| PC       | Pdgfrb            | NM_008809                     | 905            | 540   | 1.68                      |
|          | Cspg4 (NG2)       | NM_139001                     | 10             | 35    | 0.29                      |
|          | Mcam (CD146)      | NM_023061                     | 57             | 31    | 1.82                      |
|          | Rgs5              | NM_009063                     | 9              | 16    | 0.60                      |
|          | Des               | NM_010043                     | 31             | 27    | 1.17                      |
|          | Ngfb              | NM_013609                     | 159            | 142   | 1.12                      |
|          | Angpt1            | NM_009640                     | 76             | 150   | 0.51                      |
|          | Vim               | NM_011701                     | 33064          | 29895 | 1.11                      |
| EC       | Pecam1 (CD31)     | NM_008816                     | 2              | 9     | 0.20                      |
|          | Flt1 (VEGFR1)     | NM_010228                     |                | 16    |                           |
|          | Kdr (VEGFR2)      | NM_010612                     | 60             | 38    | 1.57                      |
|          | Vwf               | NM_011708                     | 8              | 8     | 0.97                      |
|          | Sele (E-selectin) | NM_011345                     | 5              | 5     | 1.12                      |
| MSC      | Anpep (CD13)      | NM_008486                     | 227            | 256   | 0.89                      |
|          | Itgb1 (CD29)      | NM_010578                     | 3088           | 1747  | 1.77                      |
|          | Cd44              | NM_009851                     | 4              | 8     | 0.47                      |
|          | Nt5e (CD73)       | NM_011851                     | 6              | 6     | 0.99                      |
|          | Thy1 (CD90)       | NM_009382                     | 3              | 13    | 0.25                      |
|          | Eng (CD105)       | NM_007932                     | 165            | 116   | 1.42                      |
|          | Vcam1 (CD106)     | NM_011693                     | 2831           | 5406  | 0.52                      |
| NSC      | Nes               | NM_016701                     | 155            | 24    | <b>6.38</b>               |
|          | Cxcl12            | NM_013655                     | 2969           | 849   | <b>3.50</b>               |
|          | Lepr              | NM_010704                     | 87             | 103   | 0.84                      |
| Other SC | Ly6a (Sca1)       | NM_010738                     | 22387          | 6319  | <b>3.54</b>               |
|          | Cd34              | NM_133654                     | 4              | 6     | 0.56                      |

**Supplemental Table 1** Genes, GenBank Accession number, and PCR Primers.

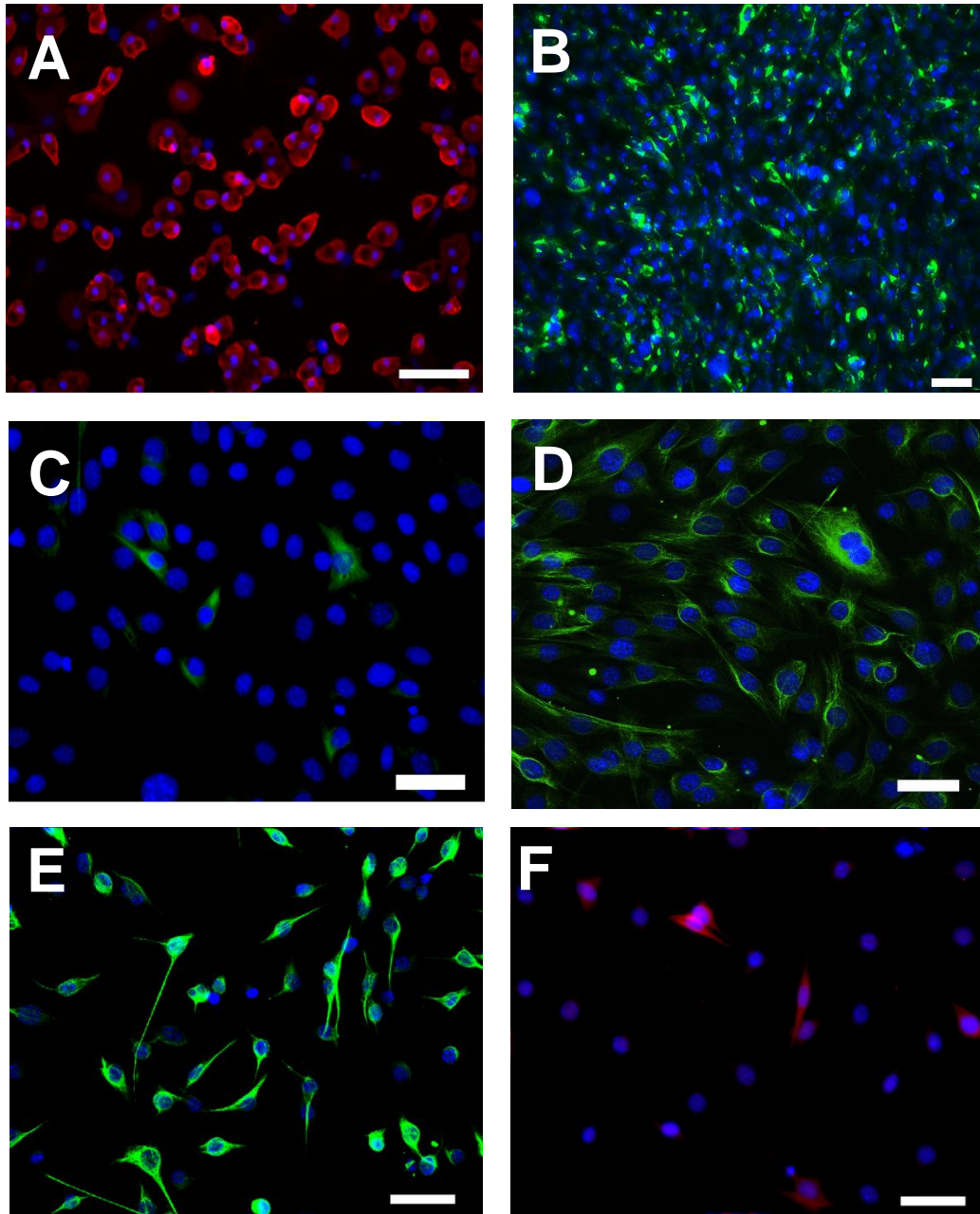
| Gene         | GeneBank accession numbers | Forward primer             | Reverse primer           |
|--------------|----------------------------|----------------------------|--------------------------|
| NG2          | NM_139001                  | TGACCTACAGGGCCACA          | TGGATGGCCACTCGGAA        |
| PDGFRb       | NM_008809                  | TGAGAGTCACCCTGCCAA         | CTCCAGGTGGAGTCGTA        |
| CD146        | NM_023061                  | CTCCCATGATGAGCGAA          | GAGGGTTGCCATCTGTCA       |
| aSMA         | NM_007392                  | ACTACTGCCGAGCGTGAGATT      | GTAGACAGCGAAGCCAAGATG    |
| Myocardin    | NM_145136                  | TGCTGCTGGGTGAAGAGA         | TGCTGGTGGAGAAGCAGA       |
| vWF          | NM_011708                  | TCGTGGAGGAGTAATCCAG        | AGCCTTGGCAAACTCTTCA      |
| Fik1(VEGFR2) | NM_010228                  | AGCGGAGACGCTTTCATAA        | GCCCCTTTGCTCTTATAGGG     |
| SM22a        | NM_011526                  | GGAGGAGCGACTAGTGA          | GCAGTTGGCTGTCTGTGA       |
| GAPDH        | NM_008084                  | TGAAGGTCGGTGTGAACGGATTTGGC | CATGTAGGCCATGAGGTCCACCAC |

## Supplemental Figure 1



**Supplemental Figure 1** Interactions between capillary endothelial cells (cECs) and capillary pericytes (cPCs) in Matrigel. cECs (DsRed; red) or cPCs (GFP; green) were incubated in Matrigel in the presence of VEGF (20 ng/ml). cECs formed endothelial tubes but cPC formed just cell clusters and small funicular structures. When cECs and cPCs were co-incubated, cPCs were distributed around the tubes made up of cECs to form capillary like structure. Scale bars, 100  $\mu$ m.

## Supplemental Figure 2



**Supplemental Figure 2** Immunofluorescence characterization of PCs. After mPCs were exposed to appropriate differentiation stimuli, cells were fixed and stained with primary antibodies against Fabp4 (**A**), osteopontin (**B**). The cells (cPC6 and mPCs) at non-differentiation condition were stained with nestin (**C** and **D**). After mPCs were incubated at neuro-maintenance medium, the staining of nestin was more enhanced (**E**). After mPCs were further exposed to neuro-differentiation medium, some of cells were stained with GFAP (**F**). Nuclei were counter stained with DAPI. Scale bars, 50  $\mu$ m.